The RP Method: A New Tool for the Iterative Solution of the Nonlinear Schrödinger Equation

Armando Vannucci, *Member, IEEE*, Paolo Serena, *Student Member, IEEE*, and Alberto Bononi

***Abstract*—An original approach to the solution of the nonlinear Schrödinger equation (NLSE) is pursued in this paper, following the *regular perturbation* (RP) method. Such an iterative method provides a closed-form approximation of the received field and is thus appealing for devising nonlinear equalization/compensation techniques for optical transmission systems operating in the nonlinear regime. It is shown that, when the nonlinearity is due to the Kerr effect alone, the order n RP solution coincides with the order $2n+1$ Volterra series solution proposed by Brandt-Pearce and co-workers. The RP method thus provides a computationally efficient way of evaluating the Volterra kernels, with a complexity comparable to that of the split-step Fourier method (SSFM). Numerical results on 10 Gb/s single-channel terrestrial transmission systems employing common dispersion maps show that the simplest third-order Volterra series solution is applicable only in the weakly nonlinear propagation regime, for peak transmitted power well below 5 dBm. However, the insight in the nonlinear propagation phenomenon provided by the RP method suggests an enhanced regular perturbation (ERP) method, which allows the first-order ERP solution to be fairly accurate for terrestrial dispersion-mapped systems up to launched peak powers of 10 dBm.**

***Index Terms*—Nonlinear systems, optical fiber communication, optical Kerr effect, optical propagation in nonlinear media.**

I. Introduction

MOST OF the research in long-haul terrestrial and submarine optical communication links today concentrates on the design and optimization of the dispersion-mapped optical fiber channel rather than the optimization of the receiver and of the modulation format. This fact has progressively increased the cultural gap between the classical communications community and the optical communications community.

The analysis of the long-haul optical channel starts from the nonlinear Schrödinger equation (NLSE) describing the field propagation in a single-mode optical fiber. Its direct numerical solution by the split-step Fourier method (SSFM) [1], as implemented in most commercially available software packages, is the key design tool available to the communications engineer. The guidelines for the design are learned most often from simplified versions of the NLSE for which an approximate analytical solution is available. Linearization around a working point is the technique that has most often been successfully employed for the study of nonlinear effects, as in the case of the study of parametric gain [2]–[4] and cross-phase modulation [5], [6]. Even in the study of dispersion-managed solitons, linearization occurs around an analytical waveform close to the actual solution, according to the variational principle [7], [8].

Linearization is used because the NLSE generally does not admit an analytical solution when both the nonlinear term and chromatic dispersion are taken into account. Notable exceptions include the search of the eigenfunctions of the NLSE, for which the exact solution is obtained by the inverse scattering method in the form of classical solitons [1], and the treatment of nonreturn-to-zero (NRZ) pulses when the chromatic dispersion is extremely small, for which a solution is obtained by the dam-breaking approximation [9]. Other studies that go beyond linearization include the application of perturbation theory to the search of the eigenfunctions of the multidimensional NLSE in the field of molecular physics [10].

Recently, Brandt-Pearce and co-workers have tackled the NLSE using a Volterra series approach [11], [12], pioneering the introduction in the long-haul optical transmission world of a well-established tool in nonlinear system theory and laying the ground for a possible renewed interest of the traditional communications community into optical communications. The value of such pioneering work is that it makes it possible to adapt known communication theory results, such as equalization techniques for nonlinear channels [13], for application to the nonlinear optical channel. However, the numerical findings in [11] and [12] are quite discouraging when applied to typical long-haul dispersion-mapped optical links, with large nonlinear cumulated phase: too many Volterra kernels are needed in the series expansion in order to obtain a good approximation of the output field for typical power levels in terrestrial systems, so that the authors in [12] were forced to use extremely low transmitted peak power levels. The main concern here is on computational complexity: a Volterra kernel of order n entails a multiple integral of order n in the frequency domain, so that the computational complexity of the Volterra expansion quickly exceeds that of the direct SSF computation.

This paper stems from the thesis work of Paolo Serena [14], who studied the approximate solution of the NLSE by the regular perturbation (RP) method [15]. Such method, summarized in Section II of this paper, provides a recursive closed-form solution that provides good insight into the nature of the nonlinear distortion and a computationally efficient numerical evaluation method.

During such thesis work, we observed the close similarity of the first-order RP solution to the Volterra series solution truncated to the third kernel, as given in [11] and [12]. Motivated by

Manuscript received May 10, 2001; revised January 31, 2002.

The authors are with the Dipartimento di Ingegneria dell'Informazione, Università di Parma, 43100 Parma, Italy (e-mail: vannucci@tlc.unipr.it).

Publisher Item Identifier 10.1109/JLT.2002.800376.

such observation, we further verified that such coincidence carries over to the fifth-order kernel. Such findings are presented in Section III of the paper. We then found a way to prove by induction that the order n RP solution coincides with the order $2n+1$ Volterra series solution, for any integer n. Appendix II contains the details of the proof.

In summary, we realized that the RP recursive solution coincides with the Volterra expansion and is thus a computationally efficient way of evaluating the Volterra kernels by avoiding multiple integrations. The conditions for convergence of the RP series expansion can also be used to prove convergence of the Volterra series expansion.

We must emphasize that the RP method does provide a gain in computational efficiency compared with the direct Volterra kernels evaluation, but not compared with the SSFM, which still provides the most computationally efficient approach. However, the RP method and the SSFM have comparable complexities, as discussed in Section IV of this paper.

Section IV tackles the issue of whether there exists a finite lumped-element block-diagram description of the nonlinear fiber, starting from its finite-order Volterra solution. Unfortunately, a negative answer is obtained from known theorems on nonlinear system theory. However, the recursive nature of the RP solution bears a similarity with the SSFM, and we found a simple connection between the two methods, which provides a good understanding of the approximations entailed by the RP expansion up to a given order, as well as an approximate block-diagram description of the nonlinear fiber, and an efficient computational algorithm for the terms of the RP solution.

In Section V of this paper, we apply the RP method to a typical 10 Gb/s single-channel dispersion-mapped 5×100 km terrestrial system and quantify the approximation error, expressed as the normalized mean-squared difference, over the whole transmission period, with respect to the "true" split-step Fourier (SSF) solution. We find that a first-order RP expansion (i.e., a third-order Volterra expansion) provides an acceptable level of accuracy up to peak transmitted powers of a few dBm, the accuracy being worse for maps whose transmission fiber has lower dispersion. In other words, the method cannot be used with typical values of peak transmitted power around 9 dBm. Switching to a second-order RP solution, i.e., fifth-order Volterra solution, improves accuracy, but the fifth-order kernel is too cumbersome to treat for any analytical computation of practical use.

Fortunately, there is a simple trick that allows a first-order RP solution to hold up to power levels of interest in terrestrial systems. We call this the enhanced regular perturbation (ERP) method, presented in Section VI of this paper. The idea is borrowed from the variational principle: because it is known that the phase of the received field will swing around the average cumulated nonlinear phase, a change of variable is made to eliminate such average nonlinear phase before applying the RP method. The results show that such a first-order ERP method gives an accurate output field description for the most common dispersion maps up to peak powers of about 10 dBm, the accuracy varying according to the in-line residual dispersion.

Finally, Section VII of this paper contains the conclusions.

II. RP Solution of the NLSE

The propagation of the optical field complex envelope $\mathcal{E}(z,t)$ $[\sqrt{W}]$ in a single-mode optical fiber is described by the NLSE [1] as follows:

$$\frac{\partial \mathcal{E}(z,t)}{\partial z} + \frac{\alpha}{2}\mathcal{E}(z,t) + \beta_1 \frac{\partial \mathcal{E}(z,t)}{\partial t} - j\frac{\beta_2}{2}\frac{\partial^2 \mathcal{E}(z,t)}{\partial t^2} + j\gamma|\mathcal{E}(z,t)|^2\mathcal{E}(z,t) = 0 \tag{1}$$

where we adopt the electrical engineers sign convention for the Fourier transform, and where α $[m^{-1}]$ is the power attenuation per unit length, $\beta_i \triangleq (d^i\beta/d\omega^i)_{\omega=\omega_0}$ is the ith coefficient of the frequency expansion of the propagation constant $\beta(\omega)$ at $\omega = \omega_0$, and γ $[W^{-1}m^{-1}]$ is the nonlinear coefficient. Equation (1) considers only Kerr nonlinearity and group velocity dispersion (GVD). The Raman effect is neglected here, as well as higher order chromatic dispersion terms, although the analysis and the results can be extended to cope with such terms as well.

We now apply the RP method, described in Appendix I, to the above equation. It is easy to recognize in (1) the structure of (36), where $N[\mathcal{E}(z,t)] = j\gamma|\mathcal{E}(z,t)|^2\mathcal{E}(z,t)$ is the only nonlinear term of the NLSE and $L[\mathcal{E}(z,t)] = 0$ the propagation equation in the linear regime, whose solution is well known. Prior to introducing the RP series expansion for the optical field envelope, the NLSE can be further simplified, as customary, by introducing a normalized field $\hat{A}(z,T)$ referred to the retarded time frame $T = t - (z/v_g)$, being that $v_g = 1/\beta_1$ is the group velocity of the field. $\hat{A}$ and $\mathcal{E}$ differ by an attenuation factor that depends on the length z of the fiber, as follows:

$$\mathcal{E}(z,T) \triangleq \hat{A}(z,T)e^{-(\alpha/2)z}. \tag{2}$$

The simplified NLSE then reads

$$\frac{\partial \hat{A}(z,T)}{\partial z} = j\frac{\beta_2}{2}\frac{\partial^2 \hat{A}(z,T)}{\partial T^2} - j\gamma|\hat{A}(z,T)|^2\hat{A}(z,T)e^{-\alpha z}. \tag{3}$$

Let us now express the field $\hat{A}(z,T)$ in a power series of γ

$$\hat{A}(z,T) = \sum_{k=0}^{\infty} \gamma^k \hat{A}_k(z,T) \tag{4}$$

and insert the latter in (3): for a real γ,

$$\sum_{k=0}^{\infty} \gamma^k \frac{\partial \hat{A}_k(z,T)}{\partial z} = \sum_{k=0}^{\infty} \gamma^k j\frac{\beta_2}{2}\frac{\partial^2 \hat{A}_k(z,T)}{\partial T^2} - j\gamma \sum_{i=0}^{\infty}\sum_{n=0}^{\infty}\sum_{l=0}^{\infty} \gamma^{i+n+l} \cdot \hat{A}_i(z,T)\hat{A}_n^*(z,T)\hat{A}_l(z,T)e^{-\alpha z}. \tag{5}$$

Equating the terms that multiply equal powers of γ on both sides, we get a system of recursive linear differential equations, the kth being

$$\frac{\partial \hat{A}_k(z,T)}{\partial z} = j\frac{\beta_2}{2}\frac{\partial^2 \hat{A}_k(z,T)}{\partial T^2} - j\sum\sum_{i+n+l=k-1}\sum \cdot \hat{A}_i(z,T)\hat{A}_n^*(z,T)\hat{A}_l(z,T)e^{-\alpha z} \quad (6)$$

where, consistently with (38), the last term includes the contributions $\hat{A}_i(z,T)$ to the field with $i<k$, which are known from previous iterations.

In order to get an analytical approximation of the optical field, in most cases of practical interest it is sufficient to solve such iterative equations only for $k=0,1,2$. If the input field is $A(0,T)$, the initial condition for $k=0$ is $\hat{A}_0(0,T)=A(0,T)$, while the higher order contributions to the field have zero initial values: $\hat{A}_1(0,T)=\hat{A}_2(0,T)=0$. For $k=0$, the linear solution in the frequency domain is

$$\hat{A}_0(z,\omega) = A(0,\omega)e^{-j(\beta_2/2)\omega^2 z}. \quad (7)$$

For $k=1$, the only contribution to the triple summation in (6) comes from $i=n=l=0$, and the equation to solve is

$$\frac{\partial \hat{A}_1(z,T)}{\partial z} = j\frac{\beta_2}{2}\frac{\partial^2 \hat{A}_1(z,T)}{\partial T^2} - j\left|\hat{A}_0(z,T)\right|^2\hat{A}_0(z,T)e^{-\alpha z}. \quad (8)$$

Taking Fourier transforms and integrating with respect to z, we get the solution

$$\hat{A}_1(z,\omega) = e^{-j(\beta_2/2)\omega^2 z}(-j)\int_0^z e^{+j(\beta_2/2)\omega^2\xi}e^{-\alpha\xi} \cdot \iint \hat{A}_0(\xi,\omega_1)\hat{A}_0^*(\xi,\omega_2)\hat{A}_0(\xi,\omega-\omega_1+\omega_2) \cdot \frac{d\omega_1}{2\text{pi}}\frac{d\omega_2}{2\text{pi}}\,d\xi \quad (9)$$

where the integrals extend from $-\infty$ to ∞. For $k=2$, the equation is

$$\frac{\partial \hat{A}_2(z,T)}{\partial z} = j\frac{\beta_2}{2}\frac{\partial^2 \hat{A}_2(z,T)}{\partial T^2} - j \cdot \left(2\left|\hat{A}_0(z,T)\right|^2\hat{A}_1(z,T) + \hat{A}_0^2(z,T)\hat{A}_1^*(z,T)\right) \cdot e^{-\alpha z} \quad (10)$$

which, expressed in the frequency domain and integrated with respect to z, yields the solution

$$\hat{A}_2(z,\omega) = e^{-j(\beta_2/2)\omega^2 z}(-j)\int_0^z e^{+j(\beta_2/2)\omega^2\xi}e^{-\alpha\xi} \cdot \left(2\iint \hat{A}_0(\xi,\omega_1)\hat{A}_0^*(\xi,\omega_2) \cdot \hat{A}_1(\xi,\omega-\omega_1+\omega_2)\,d\omega_1\,d\omega_2 + \iint \hat{A}_0(\xi,\omega_1)\hat{A}_1^*(\xi,\omega_2) \cdot \hat{A}_0(\xi,\omega-\omega_1+\omega_2)\,d\omega_1\,d\omega_2\right)d\xi. \quad (11)$$

It is now necessary to insert the expression of $\hat{A}_0(z,\omega)$ into (9) in order to get an explicit dependence of $\hat{A}_1(z,\omega)$ on the input field; this must be done also for $\hat{A}_2(z,\omega)$, inserting (7) and (9) into (11). After some algebra, we get (12) and (13) shown at the bottom of the page. The second-order RP approximation to the output normalized optical field is then

$$\hat{A}(z,\omega) \approx \hat{A}_0(z,\omega) + \gamma\hat{A}_1(z,\omega) + \gamma^2\hat{A}_2(z,\omega) \quad (14)$$

and we note that the GVD term $e^{-j(\beta_2/2)\omega^2 z}$ appears in all terms. The great value of (7), (12), and (13) is that they provide a closed-form approximation of the output field. Such equations will be related to the Volterra series solution of the NLSE in the next section of this paper.

$$\hat{A}_1(z,\omega) = \exp[-j(\beta_2/2)\omega^2 z](-j)\iint \cdot\left[\int_0^z \exp\left[-\alpha + j(\beta_2/2)(\omega^2-\omega_1^2+\omega_2^2-(\omega-\omega_1+\omega_2)^2)\right]\xi\,d\xi\right] \cdot A(0,\omega_1)A^*(0,\omega_2)A(0,\omega-\omega_1+\omega_2)\,d\omega_1\,d\omega_2 \quad (12)$$

$$\hat{A}_2(z,\omega) = \exp[-j(\beta_2/2)\omega^2 z]\iiiint \cdot\left[-2\int_0^z \exp\left[-\alpha + j\frac{\beta_2}{2}(\omega^2-\omega_1^2+\omega_2^2-(\omega-\omega_1+\omega_2)^2)\right]\xi \cdot\left(\int_0^\xi \exp\left(\left[-\alpha + j\frac{\beta_2}{2}\left((\omega-\omega_1+\omega_2)^2-\omega_3^2+\omega_4^2-(\omega-\omega_1+\omega_2-\omega_3+\omega_4)^2\right)\right]\mu\right)d\mu\right)d\xi + \int_0^z \exp\left(\left[-\alpha + j\frac{\beta_2}{2}\left(\omega^2-\omega_1^2+(\omega_2-\omega_3+\omega_4)^2-(\omega-\omega_1+\omega_2-\omega_3+\omega_4)^2\right)\right]\xi\right) \cdot\left(\int_0^\xi \exp\left(\left[-\alpha + j\frac{\beta_2}{2}\left(\omega_2^2-\omega_3^2+\omega_4^2-(\omega_2-\omega_3+\omega_4)^2\right)\right]\mu\right)d\mu\right)d\xi\right] \cdot A(0,\omega_1)A^*(0,\omega_2)A(0,\omega_3)A^*(0,\omega_4)A(0,\omega-\omega_1+\omega_2-\omega_3+\omega_4) \cdot d\omega_1\,d\omega_2\,d\omega_3\,d\omega_4. \quad (13)$$

III. Relation to the Volterra Series Approach

An approximate analytical solution to the NLSE has already been studied in the literature through the use of Volterra series [11]. To briefly summarize the results of this method, the NLSE (1) must be rewritten in the frequency domain, using the retarded and attenuated[1] optical field $A(z, T) \triangleq \mathcal{E}(z, t - \beta_1 z)$ as follows:

$$\frac{\partial A(z,\omega)}{\partial z} = G_1(\omega)A(z,\omega) + \iint G_3(\omega_1, \omega_2, \omega - \omega_1 + \omega_2) \cdot A(z,\omega_1)A^*(z,\omega_2)A(z,\omega-\omega_1+\omega_2)\,d\omega_1\,d\omega_2 \quad (15)$$

where we set $G_1(\omega) \triangleq -(\alpha/2) - j(\beta_2/2)\omega^2$ and $G_3(\omega_1, \omega_2, \omega_3) \triangleq -j\gamma$. One then postulates a solution in the form of a truncated Volterra series. The fifth-order solution reads

$$\begin{aligned} &A(z,\omega) \\ &= H_1(\omega, z)A(0,\omega) + \iint H_3(\omega_1,\omega_2,\omega-\omega_1+\omega_2,z) \\ &\quad \cdot A(0,\omega_1)A^*(0,\omega_2)A(0,\omega-\omega_1+\omega_2)\,d\omega_1\,d\omega_2 \\ &\quad + \iiiint H_5(\omega_1,\omega_2,\omega_3,\omega_4,\omega-\omega_1+\omega_2-\omega_3+\omega_4,z) \\ &\quad \cdot A(0,\omega_1)A^*(0,\omega_2)A(0,\omega_3)A^*(0,\omega_4) \\ &\quad \cdot A(0,\omega-\omega_1+\omega_2-\omega_3+\omega_4)\,d\omega_1\,d\omega_2\,d\omega_3\,d\omega_4 \end{aligned} \quad (16)$$

where $H_i(\cdot, z)$ are the Volterra kernels. Even order terms of the series must be identically zero due to the absence of second-order nonlinearities in the NLSE. Plugging (16) in both sides of (15), terms of first, third and fifth order appear on both sides, while terms of seventh and ninth order appear only on the right-hand side (RHS). It is then apparent that an expression in the form of (16) will never be an exact solution of the NLSE. More precisely, one can show that a polynomial equation such as (15) will never admit an exact solution expressed, through the initial conditions, as a polynomial of finite order. Nevertheless, in the assumption of a sufficiently small input field, we can neglect higher order terms and equate the terms of first, third and fifth order, and then get a set of differential equations for the Volterra kernels [11, eqs. (7)–(9)] that must be solved with initial conditions $H_1(\omega, 0) = 1$, $H_3(\omega_1, \omega_2, \omega_3, 0) = 0$ and $H_5(\omega_1, \omega_2, \omega_3, \omega_4, \omega_5, 0) = 0$ [11], as per (16). The general solution for the first-order kernel [11, eq. (10)] can be applied to our case through the definitions of G_1 and G_3 as follows:

$$H_1(\omega, z) = e^{G_1(\omega)z} = e^{-(\alpha/2)z}e^{-j(\beta_2/2)\omega^2 z} \quad (17)$$

which coincides with the linear fiber frequency response. For the third-order kernel, the general solution [11, eq. (11)] specializes to this case as follows:

$$H_3(\omega_1, \omega_2, \omega-\omega_1+\omega_2, z) = e^{-(\alpha/2)z}e^{-j(\beta_2/2)\omega^2 z}(-j\gamma) \cdot \left[\frac{1 - e^{[-\alpha - j(\beta_2/2)[(\omega-\omega_1+\omega_2)^2 - (\omega^2-\omega_1^2+\omega_2^2)]]z}}{\alpha + j(\beta_2/2)[(\omega-\omega_1+\omega_2)^2-(\omega^2-\omega_1^2+\omega_2^2)]}\right]. \quad (18)$$

Note that for large fiber length z, the exponential term in the numerator in (18) can be neglected with respect to 1. Also, for large GVD fibers, one could be tempted to drop the α term in the denominator, as done, e.g., in [16] in the analysis of the efficiency of four-wave mixing. However, dealing with signals with a continuous spectrum, α cannot in general be neglected for all significant frequency bands of the signal.

The general solution for the fifth-order kernel, reported in [11, eqs. (12) and (13)], specializes to this case, as shown in (19) at the bottom of the page. Instead of directly applying [11, eqs. (12) and (13)] to this case, the following changes of the ω_i variables

[1]Here the notation of [11] is kept for the purpose of comparison.

$$\begin{aligned} &H_5(\omega_1,\omega_2,\omega_3,\omega_4,\omega_5,z) \\ &= e^{-(\alpha/2)z}e^{-j(\beta_2/2)\omega^2 z}(\gamma^2) \cdot \left[\frac{e^{[-2\alpha + j(\beta_2/2)((\omega_1-\omega_2+\omega_3-\omega_4+\omega_5)^2-\omega_1^2+\omega_2^2-\omega_3^2+\omega_4^2-\omega_5^2)]z} - 1}{\left[-2\alpha + j\,\frac{\beta_2}{2}\,((\omega_1-\omega_2+\omega_3-\omega_4+\omega_5)^2-\omega_1^2+\omega_2^2-\omega_3^2+\omega_4^2-\omega_5^2)\right]}\right. \\ &\quad \cdot \left(\frac{-2}{\left[-\alpha + j\,\frac{\beta_2}{2}\,((\omega_3-\omega_4+\omega_5)^2-\omega_3^2+\omega_4^2-\omega_5^2)\right]} + \frac{+1}{\left[-\alpha + j\,\frac{\beta_2}{2}\,(\omega_2^2-\omega_3^2+\omega_4^2-(\omega_2-\omega_3+\omega_4)^2)\right]}\right) \\ &\quad - \frac{(-2)}{\left[-\alpha + j\frac{\beta_2}{2}\,((\omega_3-\omega_4+\omega_5)^2-\omega_3^2+\omega_4^2-\omega_5^2)\right]} \\ &\quad \cdot \frac{e^{[-\alpha + j(\beta_2/2)((\omega_1-\omega_2+\omega_3-\omega_4+\omega_5)^2-\omega_1^2+\omega_2^2-(\omega_3-\omega_4+\omega_5)^2)]z} - 1}{\left[-\alpha + j\frac{\beta_2}{2}\,((\omega_1-\omega_2+\omega_3-\omega_4+\omega_5)^2-\omega_1^2+\omega_2^2-(\omega_3-\omega_4+\omega_5)^2)\right]} \\ &\quad - \frac{(+1)}{\left[-\alpha + j\frac{\beta_2}{2}\,(\omega_2^2-\omega_3^2+\omega_4^2-(\omega_2-\omega_3+\omega_4)^2)\right]} \\ &\quad \left. \cdot \frac{e^{[-\alpha + j(\beta_2/2)((\omega_1-\omega_2+\omega_3-\omega_4+\omega_5)^2-\omega_1^2+(\omega_2-\omega_3+\omega_4)^2-\omega_5^2)]z} - 1}{\left[-\alpha + j\,\frac{\beta_2}{2}\,((\omega_1-\omega_2+\omega_3-\omega_4+\omega_5)^2-\omega_1^2+(\omega_2-\omega_3+\omega_4)^2-\omega_5^2)\right]}\right]. \end{aligned} \quad (19)$$

have been introduced in deriving (19): in the last term of both cited equations, ω_2 is swapped with ω_4, and a circular left shift is applied to the sequence $(\omega_1, \omega_3, \omega_5)$. Such changes do not affect the overall result of the quadruple integral in (16).

One can now directly check that the fifth-order Volterra solution (16) coincides with the second-order RP solution of the last section. In fact, one can verify that the integral in the square brackets of (12) coincides with the term in square brackets of (18), and that the double integrals in the square brackets of (13) coincide with the expression in the large square brackets of (19). The actual output optical field found through the RP method differs from the expression (14) by an attenuation term $e^{-(\alpha/2)z}$, by which $\hat{A}(z, \omega)$ must be multiplied, according to (2). Thus, it is easily seen that the linear terms (attenuation and GVD) and the terms in γ appearing in (17)–(19) are also present in the RP solution and that the two solutions coincide.

In Appendix II, it is proven by induction that the two methods yield the same solution to any order. Such coincidence is noteworthy, because the RP method seeks a solution in the form of a power series of γ, whereas the Volterra series is a generalized Taylor power series of the input field. Such coincidence is reminiscent of the coincidence of the RP method with the functional iteration method cited in [15, note 5, p. 531]. Once the coincidence of the two solutions is established, the convergence of the infinite Volterra series to the exact solution of the NLSE is equivalent to the convergence of the infinite RP series: known convergence conditions for one method can be used to prove convergence for the other.

IV. Relation to the Split-Step Fourier Method: A Parallel Fiber Model

The Volterra series approach is a powerful tool for modeling nonlinear systems. For a lumped-elements system, the Volterra kernels can be derived from its block diagram, as has been done for nonlinear radio links [17], [18], where a memoryless nonlinear amplifier is sandwiched between linear filters. The reverse problem is nontrivial: given the Volterra kernels of the previous section, is there a finite lumped-elements system described by those kernels, i.e., having the same input–output relationship? In order to answer this question, we resorted to nonlinear systems *realization theory*. Based on the results illustrated in [19], it is possible to prove that the kernels derived for the nonlinear fiber are not suitable for modeling a *bilinear system*, i.e., one with a finite block diagram, because, for instance, the denominator of the third-order kernel in (18) is not factorizable in the product of three functions, each depending on a single variable ω_i, and thus, in the terminology of [19], $H_3(\cdot)$ is not a *recognizable* function. However, we will provide below an infinite block diagram schematic of the nonlinear fiber by working on the RP solution.

The first advantage of the RP solution with respect to the Volterra solution is its computational simplicity. In fact, the evaluation of the optical field through the truncated Volterra series is extremely computationally expensive, the third- and fifth-order kernels requiring the evaluation of double and quadruple integrals in the frequency domain, respectively. We wish to now show that the RP method has the complexity of a single integration in the spatial coordinate z. Let us rewrite the equations in (7), (9) and (11) reintroducing the attenuation terms, thus using attenuated optical fields $A_i(z, \omega)$ instead of $\hat{A}_i(z, \omega)$ and substituting the convolutions in ω with the Fourier transform of products in the time domain, shown in (20)–(22) at the bottom of the page where $\mathcal{F}$ denotes the Fourier transform. The above terms can be computed by a simple algorithm: a cycle that scans the fiber in finite steps from $\xi = 0$ to $\xi = z$, storing and updating the result of the integrals in (21) and (22) in two scalar variables. At each step, the linear contribution $A_0(\xi, \omega)$ is computed from (20) and the integral in (21) is updated, using direct and inverse Fourier transforms to switch between time and frequency domains, to yield an updated $A_1(\xi, \omega)$. Similarly, using (22), $A_2(\xi, \omega)$ also can be updated at the same step.

The algorithm just described bears a strong resemblance with the SSFM, both because it scans the fiber along its length and because of its intensive use of Fourier transforms. Despite such similarity, the present algorithm does not aim at directly solving the NLSE, but only at computing the RP solution of second order, and it can in principle be extended to higher orders. Thus, to establish the accuracy of the solution, both the *step size* used to scan the fiber length, as in the SSFM, and the order of the RP method are important parameters.

Let $H_\xi(\omega) = e^{-((\alpha/2)+j(\beta_2/2)\omega^2)\xi}$ be the transfer function of a linear fiber of length ξ. Equation (21) can be written as

$$A_1(z,\omega) = (-j)\int_0^z H_{z-\xi}(\omega)\mathcal{F}\left[|A_0(\xi,T)|^2 A_0(\xi,T)\right] d\xi \tag{23}$$

where a linear filtering with a fiber of length $z - \xi$ is applied in the integrand, and the terms appearing in the Fourier transform are, according to (20), $A_0(\xi, \omega) = H_\xi(\omega)A(0, \omega)$, i.e., the result of filtering the input field with a linear fiber of length ξ, complementary to $z - \xi$. A discretization of the integral in (23), with step Δ, suggests that the resulting field $A(z, \omega) \approx A_0(z, \omega) + \gamma A_1(z, \omega)$ can be thought of as the output of the block diagram depicted in Fig. 1.

$$A_0(z,\omega) = e^{-((\alpha/2)+j(\beta_2/2)\omega^2)z} A(0,\omega) \tag{20}$$

$$A_1(z,\omega) = e^{-((\alpha/2)+j(\beta_2/2)\omega^2)z}(-j)\int_0^z e^{+((\alpha/2)+j(\beta_2/2)\omega^2)\xi}\mathcal{F}\left[|A_0(\xi,T)|^2 A_0(\xi,T)\right] d\xi \tag{21}$$

$$A_2(z,\omega) = e^{-((\alpha/2)+j(\beta_2/2)\omega^2)z}(-j)\int_0^z e^{+((\alpha/2)+j(\beta_2/2)\omega^2)\xi}\mathcal{F}\left[2|A_0(\xi,T)|^2 A_1(\xi,T) + A_0^2(\xi,T)A_1^*(\xi,T)\right] d\xi \tag{22}$$

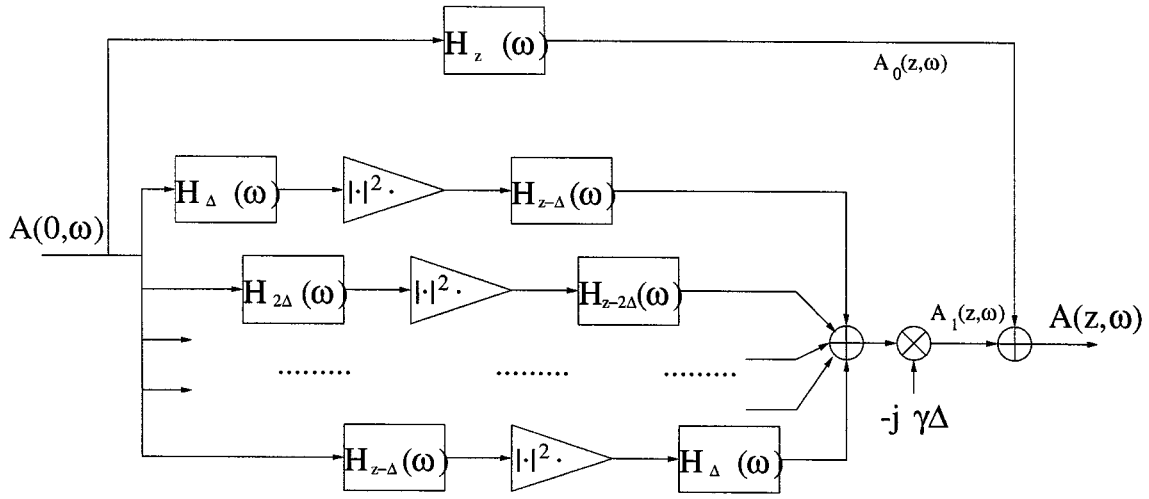

Fig. 1. A parallel fiber model derived from the first-order RP method.

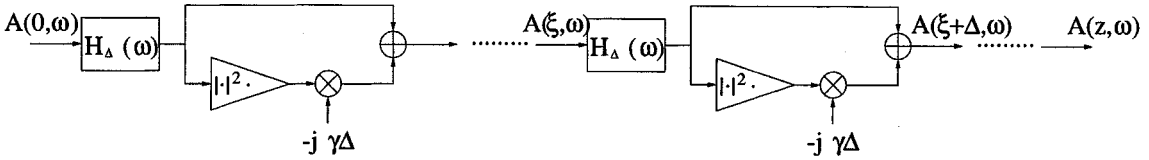

Fig. 2. A serial fiber model derived from the SSFM.

Let us now recall the strategy adopted by the SSFM to solve the NLSE. The fiber is split in slices of size Δ. The linear filtering and nonlinear distortion effects are successively applied at each step by considering the linear and nonlinear contributions to the NLSE separately. At position $z = \xi$, one can first apply the linear operator to obtain an updated field

$$\begin{aligned}\tilde{A}(\xi+\Delta,\,\omega) &= e^{(-(\alpha/2)-j(\beta_2/2)\omega^2)\Delta}A(\xi,\,\omega)\\ &= H_\Delta(\omega)A(\xi,\,\omega)\end{aligned} \tag{24}$$

and then the nonlinear operator to get the output field

$$\begin{aligned}A(\xi+\Delta,\,T) &= \tilde{A}(\xi+\Delta,\,T)e^{-j\gamma|\tilde{A}(\xi+\Delta,\,T)|^2\Delta}\\ &\approx \tilde{A}(\xi+\Delta,\,T)\left[1-j\gamma\left|\tilde{A}(\xi+\Delta,\,T)\right|^2\Delta\right]\end{aligned} \tag{25}$$

where the last line includes a first-order expansion of the exponential, valid for $\Delta \to 0$. From a system perspective, the successive application of (24) and (25) results in the schematic of Fig. 2.

Referring to Fig. 2, the input field can travel along different paths to reach the output. At each step, it can be either solely linearly filtered, when passing through the upper branches, or filtered and nonlinearly distorted, when passing through the lower branches. Thus, the output field consists of the sum of many contributions, each associated to a unique path through a concatenation of linear and nonlinear blocks. The top branch of Fig. 1 represents the linearly filtered output field $A_0(z,\,\omega)$, corresponding to the path of all upper branches of Fig. 2. It is also easy to see that each remaining branch in Fig. 1 corresponds to a path in Fig. 2 composed of all linear blocks, except for a single "descent" to a nonlinear block at coordinate $z = \xi$. Similarly, referring to (22), it can be proven that the second term of the RP method $\gamma^2 A_2(z,\,\omega)$ (coinciding with the term including the fifth-order Volterra kernel) includes the contribution of paths composed of a concatenation of linear blocks, except for a double "descent" to the nonlinear blocks at two generic coordinates along the fiber. The proof follows. Suppose that at coordinate $z = \xi$ there has been exactly one descent to a lower branch, at a previous stage $z < \xi$. Thus, the field $A(\xi,\,T) = A_0(\xi,\,T) + \gamma A_1(\xi,\,T)$ consists of a linear field A_0 and of the many *one-step* nonlinearly distorted fields that build up $A_1(\xi,\,\omega)$, as per (23). Therefore, at the second descent to a lower branch, at stage $z = \xi$, the output of the nonlinear branch in Fig. 2 is

$$\begin{aligned}&-j\gamma\Delta|A(\xi,\,T)|^2A(\xi,\,T)\\ &\quad= \gamma(-j\Delta)|A_0(\xi,\,T)|^2A_0(\xi,\,T)\\ &\qquad+\gamma^2(-j\Delta)\left[2|A_0(\xi,T)|^2A_1(\xi,T)+A_0^2(\xi,T)A_1^*(\xi,T)\right]\\ &\qquad+\gamma^3(-j\Delta)\left[2|A_1(\xi,T)|^2A_0(\xi,T)+A_1^2(\xi,T)A_0^*(\xi,T)\right]\\ &\qquad+\gamma^4(-j\Delta)|A_1(\xi,\,T)|^2A_1(\xi,\,T).\end{aligned} \tag{26}$$

By comparison with the Fourier terms in (21) and (22), it can be realized that the first term in (26) will contribute to $A_1(\xi+\Delta,\,T)$ and the second will contribute to $A_2(\xi+\Delta,\,T)$. The remaining terms will contribute to $A_3(\cdot)$ and $A_4(\cdot)$.

Extending this reasoning, one can see that the application of the order-M RP method results from the SSFM with a linearization of the exponential self-phase term (25), when the nonlinear distortion included in the NLSE is applied at M blocks only of the fiber, and terms in γ^K, with $K > M$, are neglected. Since $A_1(\xi,\,\omega)$ is a term of the third power of the input field, the four

terms in (26) will also contribute to the Volterra series terms including kernels of third, fifth, seventh and ninth order, respectively.

V. Simulation Results

To test the accuracy of the computational models illustrated above, the optical field output from four different transmission systems is evaluated by considering a typical 5×100 km terrestrial link, composed of five cascaded spans, each consisting of 100 km of transmission fiber (TF), followed by a dual-stage noiseless amplifier. A compensating fiber (CF) is sandwiched between the two amplifiers of each dual stage, and its length (common to all spans) is allowed to vary so that the residual dispersion per span D_r can be managed as a free system parameter. The gain of the dual-stage amplifier recovers all the span losses, so that the power launched in each TF equals the (peak) transmitted power $P_{\rm TX}$. The input to the compensating fiber has a fixed peak power level equal to -3 dBm, in order to avoid nonlinearity in the CF. The TF and CF are chosen among the fiber types of standard *single-mode fiber* (SMF), *dispersion compensating fiber* (DCF), *large effective area fiber* (LEAF), and *nonzero dispersion shifted fibers* (NDSF) with positive dispersion (NDSF $+$) or negative dispersion (NDSF$-$), in order to realize one of the following dispersion maps: i) SMF/DCF; ii) LEAF/DCF; iii) NDSF$+$/DCF; iv) NDSF$-$/SMF. The values of the parameters of interest, for the different fiber types, are reported in Table I.

The accuracy of the RP approximation with respect to the "true" solution obtained by the SSFM is evaluated by the *normalized square deviation* (NSD) [11], defined as

$$\mathrm{NSD} = \left(\int |A_{\rm SSFM}(z,T) - A_{\rm RP}(z,T)|^2 \, dT \right) \cdot \left(\int |A_{\rm SSFM}(z,T)|^2 \, dT \right)^{-1} \tag{27}$$

where the integrals extend to the whole transmission period, and $A_{\rm SSFM}$ is the field evaluated using the SSFM. $A_{\rm RP}$ is the field evaluated using the *first-order* RP method: $A_{\rm RP}(z,\omega) = A_0(z,\omega) + \gamma A_1(z,\omega)$. A_0 and A_1 are calculated from (20) and (23), and $A_{\rm RP}$ is updated at each span. Such approximation corresponds to a third-order Volterra solution, as discussed in Section III of this paper. The input field is a 10 Gb/s chirpless NRZ signal modulated by a pseudorandom bit sequence (PRBS) of length 64 b, filtered by a Gaussian filter with one-sided bandwidth equal to $(6/\pi)R \simeq 20$ GHz, where R is the bit rate.

For evaluating $A_{\rm SSFM}(z,T)$, the commercial software *BroadNeD*[2] was used for the simulation of optical transmission systems; for computing $A_{\rm RP}(z,T)$, we developed our own *Matlab* code. Such code implements the algorithm described in Section IV of this paper, using a step size $\Delta = 0.2$ km for performing the integral in (23) and using 1024-points Fourier transforms. A slight modification of such code was also used in deriving the results shown in Section VI. As for the computational complexity of the RP method, the run times for computing $A_{\rm RP}$ are 30% longer than those for computing $A_{\rm SSFM}$ on the same machine. We must note, however, that *Matlab* is an interpreted, rather than compiled, language and that the source code was not optimized.

[2]BroadNeD, BNeD Broadband Network Design, Inc., Berlin, Germany, and the Massachusetts Institute of Technology, Cambridge.

TABLE I
Parameters of Interest for the Fiber Types Employed in the Four Tested Dispersion Maps. Attenuation α, Dispersion D (Measured at 1550 nm Wavelength,) and Nonlinear Coefficient γ

	SMF	DCF	LEAF	NZDSF+	NZDSF-
α $[dB/km]$	0.19	0.6	0.21	0.2	0.21
D $[ps/nm/km]$	17	-100	4.4	2.9	-2.6
γ $[1/(W \cdot km)]$	1.3	5.5	1.6	2.2	1.9

The NSD can be interpreted as the relative time-averaged power of the error field associated with the RP method. In Fig. 3(a)–(d), we plot the NSD computed for the four dispersion maps described previously, versus both the residual dispersion per span D_r and the peak transmitted power $P_{\rm TX}$. D_r is varied in the range (-100, 300) [ps/nm/span] (except for the NDSF+/DCF dispersion map, where, even with a zero-length compensation fiber, D_r cannot reach the upper limit), while P_{TX} lies in the range (5, 17) [dBm]. Using such power levels, we can check the validity of the RP approximation in the moderately to highly nonlinear propagation regimes, where such approximation eventually fails to predict the output field correctly, as evidenced by the "explosion" of the NSD in Fig. 3 for large powers. From the same figure, it is apparent that a first-order RP method yields a relative error power below 1% only in the moderately nonlinear regime, where $P_{\rm TX}$ is less than 5 to 8 [dBm], depending on the dispersion map. As is well known, nonlinear effects are enhanced—and thus NSD is larger—in low-dispersion transmission fibers, such as NDSF.

To give the reader a feeling of the meaning of the NSD values in Fig. 3, Fig. 4 reports the received power waveforms at the link output both with the RP and the SSFMs for $D_r = 100$ [ps/nm/span] and $P_{\rm TX} = 8$ [dBm]: such operating points are marked with a filled circle in Fig. 3. The power profiles of Fig. 4(a)–(d) are plotted in the same 16-b time frame, and the corresponding NSD is marked in the figure.

The RP method does not entail systematic errors because simulations with a very low transmitted power such as 10^{-10} [W] provide excellent accuracy (NSD $= 10^{-20}$). However, we note from Fig. 4 that although the RP method seems to well predict the shape of the output field power, it overestimates the output power levels, especially on wider pulses, corresponding to the transmission of consecutive marks. Such overestimation is enhanced for low-dispersion NDSF transmission fibers, notwithstanding the accuracy of the predicted output power shape. These results are consistent with the observation in [11] that the Volterra series approximation is not suitable for modeling fiber nonlinearities for large pulse widths, and we provide a thorough explanation of this fact in the following section of this paper.

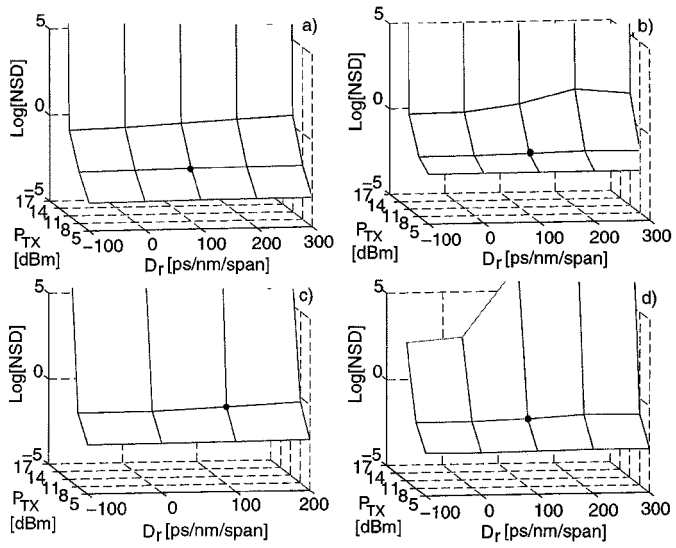

Fig. 3. Logarithmic plot of NSD versus input peak power $P_{\rm TX}$ and residual dispersion per span D_r, for a 5 × 100-km dispersion-managed link. Dispersion maps with dual-stage amplification. (a) SMF/DCF. (b) LEAF/DCF. (c) NDSF+/DCF. (d) NDSF−/SMF.

VI. The Enhanced RP Method

Consider, as a limiting case, the transmission of a field $A(0, T)$ over a zero-dispersion fiber. Using (20)–(22), the second-order RP method yields the solution

$$A_{\rm RP}(z, T) = e^{-(\alpha/2)z}\left[A(0, T) - j\gamma|A(0, T)|^2 A(0, T) \cdot L_{\rm eff}(z) - \gamma^2|A(0, T)|^4 A(0, T)\tfrac{1}{2}L_{\rm eff}^2(z)\right] \quad (28)$$

where $L_{\rm eff}(z) \triangleq \int_0^z e^{-\alpha\xi}\,d\xi$ is the fiber effective length. We recognize in (28) the Taylor series expansion, to second order in γ, of the exact solution for the output field:

$$A_E(z, T) = e^{-(\alpha/2)z}A(0, T)e^{-j\gamma|A(0, T)|^2 L_{\rm eff}(z)}. \quad (29)$$

Because nonlinear distortion acts only as a self-phase modulation term in (29), the output power is $e^{-\alpha z}|A(0, T)|^2$; such value is overestimated by (28), the relative error growing with the fifth power of the instantaneous field.

One way to mitigate this discrepancy is to postulate, as commonly done in the perturbative analysis of parametric gain [3], a solution of the NLSE of the form

$$A(z, T) \triangleq A_P(z, T)e^{-j\gamma P_0 L_{\rm eff}(z)} \quad (30)$$

where P_0 is the peak input power, which factors out the nonlinear cumulated phase from the solution.[3] The NLSE can be recast for the field A_P (including the fiber attenuation) as

$$\frac{\partial A_P(z, T)}{\partial z} = -\frac{\alpha}{2}A_P(z, T) + j\frac{\beta_2}{2}\frac{\partial^2 A_P(z, T)}{\partial T^2} - j\gamma\left(|A_P(z, T)|^2 - P_0 e^{-\alpha z}\right)A_P(z, T). \quad (31)$$

[3]During the revision of the present paper, we became aware that an alternative approach was taken in [20] to address the same problem.

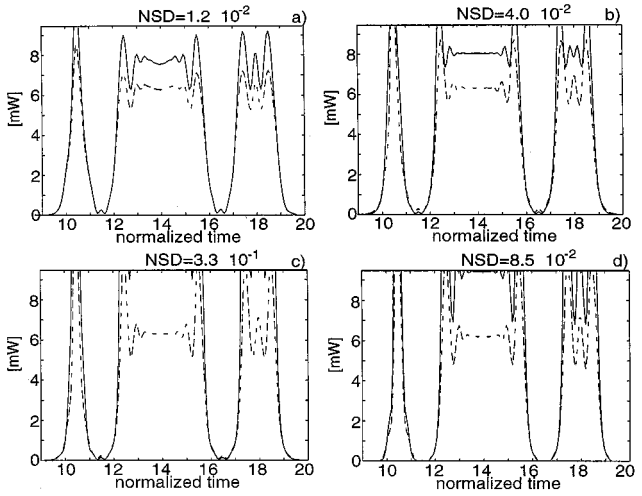

Fig. 4. Output power obtained from SSF (dashed line) and RP (solid line) methods for the same dispersion maps of Fig. 3(a)–(d). The point of operation is $D_r = 100$ [ps/nm/span], $P_{\rm TX} = 8$ [dBm].

This equation can still be solved through the RP method: calculations similar to those performed in Sections II and IV of this paper provide the first three terms for the RP approximation to A_P

$$A_{P0}(z, \omega) = e^{-((\alpha/2)+j(\beta_2/2)\omega^2)z}A_P(0, \omega) \quad (32)$$

$$A_{P1}(z, \omega) = e^{-((\alpha/2)+j(\beta_2/2)\omega^2)z}(-j)\int_0^z e^{+((\alpha/2)+j(\beta_2/2)\omega^2)\xi} \cdot \mathcal{F}\left[\left(|A_{P0}(\xi, T)|^2 - P_0 e^{-\alpha\xi}\right)A_{P0}(\xi, T)\right]d\xi \quad (33)$$

$$A_{P2}(z, \omega) = e^{-((\alpha/2)+j(\beta_2/2)\omega^2)z}(-j)\int_0^z e^{+((\alpha/2)+j(\beta_2/2)\omega^2)\xi} \cdot \mathcal{F}\left[\left(2|A_{P0}(\xi, T)|^2 - P_0 e^{-\alpha\xi}\right)A_{P1}(\xi, T) + A_{P0}^2(\xi, T)A_{P1}^*(\xi, T)\right]d\xi \quad (34)$$

with $A_P(0, \omega)$ coinciding with $A(0, \omega)$, from (30). The global approximation to the output field is found by plugging $A_P(z, T) = A_{P0}(z, T) + \gamma A_{P1}(z, T) + \gamma^2 A_{P2}(z, T)$ in (30): we will call such solution the *enhanced RP* (ERP) method.

In the case $\beta_2 = 0$, the second-order ERP method from (30) and (32)–(34) yields

$$A_{\rm ERP}(z, T) = e^{-(\alpha/2)z}\left[A(0,T) - j\gamma\left(|A(0,T)|^2 - P_0\right)A(0,T)L_{eff}(z) - \gamma^2\left(|A(0,T)|^2 - P_0\right)^2 A(0,T)\tfrac{1}{2}L_{eff}^2(z)\right]e^{-j\gamma P_0 L_{eff}(z)}. \quad (35)$$

Comparing (35) with (29), it is easily seen how the ERP approximation is close to the exact solution, both in magnitude and phase, when the input field magnitude approaches its peak level $\sqrt{P_0}$.

Fig. 5 shows, in the same frame of reference of Fig. 3, the NSD evaluated by applying the ERP method. It is seen that a significant reduction of the NSD is obtained for all maps.

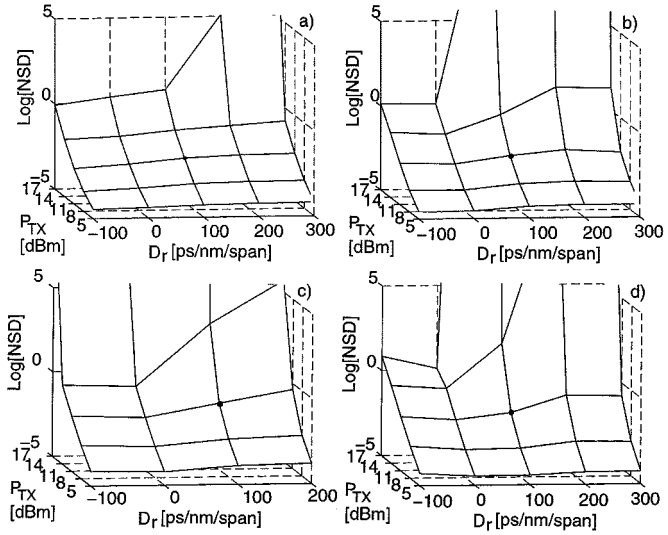

Fig. 5. Logarithmic plot of NSD versus input peak power $P_{\rm TX}$ and residual dispersion per span D_r, using the ERP method. Same systems as in Fig. 3.

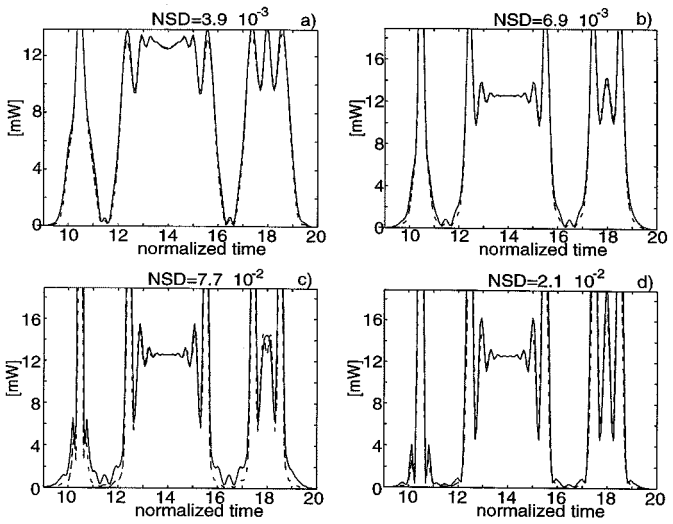

Fig. 6. Output power obtained from SSF (dashed line) and ERP (solid line) methods for the dispersion maps of Fig. 5(a)–(d). The point of operation is $D_r = 100$ [ps/nm/span], $P_{\rm TX} = 11$ [dBm].

TABLE II
PRECISION GAIN $\rm NSD_{RP}/NSD_{ERP}$ ACHIEVED BY THE ERP METHOD, FOR $D_r = 0$ AND $P_{\rm TX} = 5$, 8, 11 [dBm]. DISPERSION MAPS AS IN FIGS. 3 AND 5

	SMF/DCF	LEAF/DCF	NZDSF+/DCF	NZDSF-/SMF
$P_{TX} = 5[dBm]$	11	297	126	82
$P_{TX} = 8[dBm]$	52	182	320	151
$P_{TX} = 11[dBm]$	641	1762	10^{12}	10^{5}

Despite the fact that for the ERP method there still exists a threshold above which the $\rm NSD_{ERP}$ "explodes," a plot of $\rm NSD_{RP}/NSD_{ERP}$ (not reported here) has the same qualitative features of Figs. 5 and 3, showing that such *precision gain* increases with $P_{\rm TX}$. We report the numerical values of $\rm NSD_{RP}/NSD_{ERP}$ in Table II for all the examined dispersion maps; we consider the peak transmitted power values $P_{\rm TX} =$ 5, 8, 11 [dBm] as significant for the ERP method and disregard the minor variations along the D_r axis.

It is evident from Fig. 5 that the power threshold for the reliable application of the RP method is extended, and, as we can visually check in Fig. 6, transmitted fields with $P_{\rm TX} = 11$ [dBm] are accurately reproduced at the fiber output, thus proving the applicability of the ERP method at power levels of practical interest in terrestrial systems. Comparing Fig. 6 to Fig. 4, we note how the output power level is correctly forecast, even in the presence of long sequences of "1" bits, thus avoiding the mismatch explained in the previous section.

VII. CONCLUSION

A new approach to the solution of the NLSE has been pursued through the RP method. Based on a power series expansion of the optical field as a function of the fiber nonlinear coefficient γ, such method iteratively provides a closed-form expression for each kth term—proportional to γ^k—which approximates the field at the fiber output. The approximate solution provided by the RP method has been compared to the Volterra series transfer function method, and, though the latter is based on a different approach, we proved the coincidence of the two approximate solutions. A comparison with the SSFM has proven useful to estimate the degree of approximation involved in the RP method and to devise a new system model for the optical fiber. Such model is the sum of parallel branches, each branch being a cascade of a filter-polynomial nonlinearity-filter block.

The importance of the RP and Volterra methods is to provide closed-form approximations of the output field, thus giving an analytical insight in the nonlinear propagation phenomenon and paving the way for the development of nonlinear compensation/equalization techniques.

An algorithmic implementation of the RP method has been discussed, which has a complexity comparable to that of the widely used SSFM. A numerical comparison between these two methods shows that the optical field output from a 5×100-km terrestrial link, with several dispersion-managed maps, is correctly evaluated by a first-order RP method only at low transmitted peak powers below 5 [dBm]. ERP, an enhancement of the RP method, has been discussed and simulation results evaluated. The enhancement correctly accounts for the average nonlinear cumulated phase, thus providing a good degree of approximation in the moderately nonlinear propagation regime, with transmitted peak powers up to 10 [dBm], for all the examined dispersion-managed links.

After the submission of this work, two recent papers by Tang were published about the capacity of nonlinear dispersion-free optical channels [21], [22]. Unpublished work by the same author [22] demonstrates that much higher channel capacity can be achieved introducing fiber dispersion. However, the author notes that "extension of this work to a multispan dispersive fiber involves extremely complicated calculation of Volterra series and multidimensional integral." In view of our results, it is then plausible that the RP method can greatly simplify the numerical evaluation of the channel capacity in dispersive fiber links, within given power limits. In addition, as an object of future research, the better accuracy of the ERP method could serve to extend such results to larger transmitted powers.

APPENDIX I
THE RP METHOD

Suppose we are given a differential equation of the form

$$L[y(x)] + \epsilon N[y(x)] = 0 \tag{36}$$

where $L[\cdot]$ is a linear functional while $N[\cdot]$ is a general differential operator, linear or not, and ϵ a constant parameter. It often happens that the equation $L[y(x)] = 0$, including only the linear term, has a closed-form solution $y_0(x)$, whereas the original equation (36) does not. It is intuitive that, if the parameter ϵ is small enough, the solution of (36) will not be much different from $y_0(x)$. Let $y(x;\, \epsilon)$ be the solution of (36), coinciding with $y_0(x)$ for $\epsilon = 0$. For $\epsilon \neq 0$, one can always express the solution through a power series in ϵ:

$$y(x;\, \epsilon) = y_0(x) + \epsilon y_1(x) + \epsilon^2 y_2(x) + \cdots = \sum_{k=0}^{\infty} \epsilon^k y_k(x) \tag{37}$$

where $y_k(x)$, for $k \geq 1$, are the unknowns to be found.

This approach, known as the *regular perturbation* (RP) method (see, e.g., [15]), is suitable when the parameter ϵ is small, so that the series in (37), under certain regularity conditions for $y(x;\, \epsilon)$, converges rapidly to the true solution of (36). The unknowns can be found by inserting (37) into (36) and then equating all terms multiplying the same powers of ϵ: This way, a system of linear differential equations is obtained, the kth being

$$L[y_k(x)] + N[y_{k-1}(x),\, \ldots,\, y_0(x)] = 0 \tag{38}$$

where both $y_0(x)$ and the first $(k-1)$ functions, appearing in the argument of $N[\cdot]$, are known and we must solve for $y_k(x)$ only. The initial conditions for $y(x)$ are applied to $y_0(x)$ only, setting the initial conditions to zero for every term $y_k(x)$ with $k > 0$.

APPENDIX II
COINCIDENCE OF THE VOLTERRA AND RP SOLUTIONS

In this Appendix, we prove by induction that the RP and Volterra series solutions of the NLSE (15) coincide to any order if G_3 is proportional to γ and G_1 is not, as in the present case. This is also true when the Raman effect is included, in which case we have $G_3(\omega_1,\, \omega_2,\, \omega - \omega_1 + \omega_2) = -j\gamma(1 - \alpha_R + \alpha_R g(\omega_1 - \omega_2))$, where $g(\cdot)$ is a normalized third-order response function, and $\alpha_R \cong 0.3$ sets the relative strengths of the Kerr and Raman interactions [23]. Such property does not hold, e.g., after the change of variable in the NLSE that leads to the ERP method, in which case G_1 contains a term proportional to γ.

Consider the NLSE expressed in the form (15). The general expression of the Volterra series solution, truncated to the order $2n+1$, which includes odd-order kernels only, is

$$\begin{aligned} A^{(Vn)}(z,\, \omega) = \sum_{k=0}^{n} \int \cdots \int & H_{2k+1}(\omega_1, \omega_2, \cdots, \omega_{2k+1}, z) \\ & \cdot A(0, \omega_1) A^*(0, \omega_2) \cdots A(0, \omega_{2k+1}) \\ & \cdot d\omega_1\, d\omega_2 \cdots d\omega_{2k} \end{aligned} \tag{39}$$

where

$$\omega_{2k+1} = \omega - \omega_1 + \omega_2 - \cdots + \omega_{2k}. \tag{40}$$

The general order-n RP solution is formally simple to write:

$$A^{(RPn)}(z,\, \omega) = \sum_{k=0}^{n} \gamma^k A_k(z,\, \omega). \tag{41}$$

For the evaluation of the last kernel in (39), $H_{2n+1}(\cdot)$, we must plug (39) in the NLSE (15) and equate terms of the same order, i.e. those entailing $2n$-multiple integrals,

$$\begin{aligned} & \int \cdots \int \frac{\partial H_{2n+1}(\omega_1, \omega_2, \ldots, \omega_{2n+1}, z)}{\partial z} A(0, \omega_1) \\ & \quad \cdot A^*(0, \omega_2) \cdots A(0, \omega_{2n+1}) d\omega_1\, d\omega_2 \cdots d\omega_{2n} \\ & = \int \cdots \int G_1(\omega) H_{2n+1}(\omega_1, \omega_2, \ldots, \omega_{2n+1}, z) A(0, \omega_1) \\ & \quad \cdot A^*(0, \omega_2) \cdots A(0, \omega_{2n+1})\, d\omega_1\, d\omega_2 \cdots d\omega_{2n} \\ & \quad + \iint G_3(\omega_1, \omega_2, \omega_3) \cdot \Bigg\{ \sum_{\substack{i \\ (i+j+l=n-1)}} \sum_{j} \sum_{l} \\ & \quad \cdot \int \cdots \int H_{2i+1}(\omega_{i1}, \omega_{i2}, \ldots, \omega_{2i+1}, z) A(0, \omega_{i1}) \\ & \quad \cdot A^*(0, \omega_{i2}) \cdots A(0, \omega_{2i+1})\, d\omega_{i1}\, d\omega_{i2} \cdots d\omega_{2i} \\ & \quad \cdot \int \cdots \int H^*_{2j+1}(\omega_{j1}, \omega_{j2}, \ldots, \omega_{2j+1}, z) A^*(0, \omega_{j1}) \\ & \quad \cdot A(0, \omega_{j2}) \cdots A^*(0, \omega_{2j+1})\, d\omega_{j1}\, d\omega_{j2} \cdots d\omega_{2j} \\ & \quad \cdot \int \cdots \int H_{2l+1}(\omega_{l1}, \omega_{l2}, \ldots, \omega_{2l+1}, z) A(0, \omega_{l1}) \\ & \quad \cdot A^*(0, \omega_{l2}) \cdots A(0, \omega_{2l+1})\, d\omega_{l1}\, d\omega_{l2} \cdots d\omega_{2l} \Bigg\} d\omega_1\, d\omega_2 \end{aligned} \tag{42}$$

where ω_3 and ω_{2n+1} relate to ω as ω_{2k+1} in (40). The same relation holds between $(\omega_{2i+1},\, \omega_{2j+1},\, \omega_{2l+1})$ and $(\omega_1,\, \omega_2,\, \omega_3)$, respectively. Switching to the evaluation of the nth term $A_n(z,\, \omega)$ of the RP solution, we plug (41) in the NLSE (15) and equate the corresponding terms, i.e., those multiplying γ^n. Now, if G_3 is proportional to γ and G_1 is not, as in our case, we get

$$\begin{aligned} & \frac{\partial \gamma^n A_n(z,\, \omega)}{\partial z} \\ & \quad = G_1(\omega) \gamma^n A_n(z,\, \omega) + \iint G_3(\omega_1,\, \omega_2,\, \omega_3) \\ & \quad \cdot \sum_{\substack{i \\ (i+j+l=n-1)}} \sum_{j} \sum_{l} \left\{ \gamma^i A_i(z, \omega_1) \gamma^j A_j^*(z, \omega_2) \gamma^l A_l(z, \omega_3) \right\} \\ & \quad \cdot d\omega_1\, d\omega_2. \end{aligned} \tag{43}$$

In Section III of this paper, we analytically checked the coincidence of the first three terms of the Volterra and RP solutions. Now, assume that the corresponding terms of the solutions (39) and (41) coincide up to the order $n-1$, i.e., that

$$\begin{aligned} & \gamma^m A_m(z,\, \omega) \\ & \quad = \int \cdots \int H_{2m+1}(\omega_{m1},\, \omega_{m2},\, \ldots,\, \omega_{2m+1},\, z) \\ & \quad \cdot A(0, \omega_{m1}) A^*(0, \omega_{m2}) \cdots A(0, \omega_{2m+1}) \\ & \quad \cdot d\omega_{m1}\, d\omega_{m2} \cdots d\omega_{2m} \end{aligned} \tag{44}$$

for all $m \leq n-1$. Then, because the double integrals including $G_3(\cdot)$ in the RHS of (42) and (43) involve only indices i, j, l not exceeding $n-1$, they coincide by virtue of (44). Two expressions for such double integrals can then be obtained from (42) and (43) and equated to give

$$\begin{aligned} & e^{(+G_1(\omega)z)} \cdot \int \cdots \int \\ & \quad \cdot \frac{\partial \left(H_{2n+1}(\omega_1, \omega_2, \ldots, \omega_{2n+1}, z) \cdot e^{(-G_1(\omega)z)} \right)}{\partial z} \\ & \quad \cdot A(0,\omega_1) A^*(0,\omega_2) \cdots A(0,\omega_{2n+1})\, d\omega_1\, d\omega_2 \cdots d\omega_{2n} \\ & = e^{(+G_1(\omega)z)} \frac{\partial \left(\gamma^n A_n(z,\omega) \cdot e^{(-G_1(\omega)z)} \right)}{\partial z}. \end{aligned} \tag{45}$$

Dividing both sides by $e^{(+G_1(\omega)z)} \neq 0$, we can integrate the differential equation (45) to obtain

$$\begin{aligned} & e^{(-G_1(\omega)z)} \cdot \int \cdots \int H_{2n+1}(\omega_1, \omega_2, \cdots, \omega_{2n+1}, z) \\ & \quad \cdot A(0,\omega_1) A^*(0,\omega_2) \cdots A(0,\omega_{2n+1})\, d\omega_1\, d\omega_2 \cdots d\omega_{2n} \\ & = e^{(-G_1(\omega)z)} \cdot \gamma^n A_n(z,\omega) \end{aligned} \tag{46}$$

since, as the initial condition at $z = 0$, both functions under derivative are equal to zero, for $n > 0$. A further division of (46) by $e^{(-G_1(\omega)z)} \neq 0$ proves that (44) holds for $m = n$ as well.

REFERENCES

[1] G. P. Agrawal, *Nonlinear Fiber Optics*, 2nd ed. New York: Academic, 1995.

[2] M. Karlsson, "Modulational instability in lossy optical fibers," *J. Opt. Soc. Amer. B Opt. Phys.*, vol. 12, pp. 2071–2077, Nov. 1995.

[3] A. Carena, V. Curri, R. Gaudino, P. Poggiolini, and S. Benedetto, "New analytical results on fiber parametric gain and its effects on ASE noise," *IEEE Photon. Technol. Lett.*, vol. 9, pp. 535–537, Apr. 1997.

[4] C. Lorattanasane and K. Kikuchi, "Parametric instability of optical amplifier noise in long-distance optical transmission systems," *IEEE J. Quantum Electron.*, vol. 33, pp. 1068–1074, July 1997.

[5] A. V. T. Cartaxo, "Cross-phase modulation in intensity modulation direct detection WDM systems with multiple optical amplifiers and dispersion compensators," *J. Lightwave Technol.*, vol. 17, pp. 178–190, Feb. 1999.

[6] G. Bellotti, M. Varani, C. Francia, and A. Bononi, "Intensity distortion induced by cross-phase modulation and chromatic dispersion in optical-fiber transmissions with dispersion compensation," *IEEE Photon. Technol. Lett.*, vol. 10, pp. 1745–1747, Dec. 1998.

[7] S. K. Turitsyn and E. G. Shapiro, "Variational approach to the design of optical communication systems with dispersion management," *Opt. Fiber Technol.*, vol. 4, pp. 151–188, 1998.

[8] H. Sugahara, H. Kato, T. Inoue, A. Maruta, and Y. Kodama, "Optimal dispersion management for a wavelength division multiplexed optical soliton transmission system," *J. Lightwave Technol.*, vol. 17, pp. 1547–1559, Sept. 1999.

[9] Y. Kodama and S. Wabnitz, "Analytical theory of guiding center nonreturn to zero and return to zero signal transmission in normally dispersive nonlinear optical fibers," *Opt. Lett.*, vol. 20, pp. 2291–2293, Nov. 1995.

[10] P. R. Surján and J. Ángyán, "Perturbation theory for nonlinear time-independent Schrödinger equations," *Phys. Rev. A Gen. Phys.*, vol. 28, pp. 45–48, July 1983.

[11] K. V. Peddanarappagari and M. Brandt-Pearce, "Volterra series transfer function of single-mode fibers," *J. Lightwave Technol.*, vol. 15, pp. 2232–2241, Dec. 1997.

[12] ——, "Volterra series approach for optimizing fiber optic communications system design," *J. Lightwave Technol.*, vol. 16, pp. 2046–2055, Nov. 1998.

[13] S. Benedetto, E. Biglieri, and V. Castellani, *Digital Transmission Theory*. Englewood Cliffs, NJ: Prentice-Hall, 1987, pp. 564–574.

[14] P. Serena, "Studio teorico dell'interazione tra dispersione cromatica ed effetti non lineari nei sistemi in fibra ottica," Laurea thesis, Università degli studi di Parma, Parma, Italy, 1999.

[15] D. Zwillinger, *Handbook of Differential Equations*. Boston: Academic, 1989, pp. 528–531.

[16] M. Eiselt, "Limits on WDM systems due to four-wave mixing: A statistical approach," *J. Lightwave Technol.*, vol. 17, pp. 2261–2267, Nov. 1999.

[17] S. Benedetto, E. Biglieri, and R. Daffara, "Modeling and performance evaluation of nonlinear satellite links—A Volterra series approach," *IEEE Trans. Aerosp. Electron. Syst.*, vol. AES-15, pp. 494–507, July 1979.

[18] A. Vannucci and R. Raheli, "Optimal sequence detection based on oversampling for bandlimited nonlinear channels," in *Proc. IEEE Intern. Conf. Commun. (ICC '98)*, Atlanta, GA, June 1998, pp. 417–421.

[19] W. J. Rugh, *Nonlinear System Theory: The Volterra/Wiener Approach*. Baltimore, MD: The Johns Hopkins Univ. Press, 1981, p. 148.

[20] B. Xu and M. Brandt-Pearce, "Modified Volterra series transfer function method," *IEEE Photon. Technol. Lett.*, vol. 14, pp. 47–49, Jan. 2002.

[21] J. Tang, "The Shannon channel capacity of dispersion-free nonlinear optical fiber transmission," *J. Lightwave Technol.*, vol. 19, pp. 1104–1109, Aug. 2001.

[22] ——, "The multispan effects of Kerr nonlinearity and amplifier noises on Shannon channel capacity of a dispersion-free nonlinear optical fiber," *J. Lightwave Technol.*, vol. 19, pp. 1110–1115, Aug. 2001.

[23] K. J. Blow and D. Wood, "Theoretical description of transient stimulated Raman scattering in optical fibers," *IEEE J. Quantum Electron.*, vol. 25, pp. 2665–2673, Dec. 1989.

Armando Vannucci (S'95–M'01) was born in Frosinone, Italy, in 1968. He received the degree in electronics engineering cum laude from the University of Roma "La Sapienza," Italy, and the Ph.D. degree in information engineering from the Università di Parma, Parma, Italy in 1993 and 1998, respectively.

Until 1995, he was with the INFO-COM Department, University of Roma, conducting research activity in the field of acoustic phonetics. Since 1995, he is with the Dipartimento di Ingegneria dell'Informazione, Università di Parma. From 1995 to 1998, his research activity was in the field of nonlinear radio channels. Since 1999, his research interests are in the field of optical transmission and optical communication systems.

Paolo Serena (S'02) was born in Piacenza, Italy, in 1973. He received the degree in electronic engineering from the Università di Parma, Parma, Italy, in 1999 and has been working toward the Ph.D. degree at the university since January 2000. His main research interests include modulation instability, nonlinear propagation in optical fibers, and polarization mode dispersion.

Alberto Bononi received the degree in electronics engineering from the University of Pisa, Pisa, Italy, in 1988, and the M.A. and Ph.D degrees in electrical engineering from Princeton University, Princeton, NJ, in 1992 and 1994, respectively.

In 1990, he worked at GEC-Marconi Hirst Research Centre in Wembley, U.K., on a Marconi S.p.A. project on coherent optical systems. From 1994 to 1996, he was an Assistant Professor in the Electrical and Computer Engineering Department, SUNY Buffalo, NY, teaching courses in electric circuits and optical networks. In the Summer of 1997 and 1999, he was a Visiting Faculty at the Departement de Genie Electrique, Université Laval, QC, Canada, conducting research on fiber amplifiers. At present, he is an Associate Professor of Telecommunications at the School of Engineering,Università di Parma, Parma, Italy. He teaches courses in probability theory and stochastic processes, telecommunications networks, and optical communications. His present research interests include system design and performance analysis of high-speed all-optical networks, nonlinear fiber transmission for wavelength division multiplexing (WDM) systems, linear and nonlinear polarization mode dispersion, and transient gain dynamics in doped-fiber and Raman amplifiers.